2020 8th IEEE International Conference on Biomedical
Robotics and Biomechatronics (BioRob)
New York, USA. Nov 29 - Dec 1, 2020

Bio-Inspired Gaze-Driven Robotic Neck Brace

Biing-Chwen Chang[1], Haohan Zhang[1], Emilio Trigili[2], and Sunil K. Agrawal[1]

***Abstract*— People coordinate their eyes and head during typical activities of daily life. Subjects with poor head-eye coordination find it difficult to make eye contact with others, limiting their social interaction. Inspired by the natural vestibulo-ocular reflex (VOR) during head-eye coordination, we propose a gaze control interface to drive a robotic neck brace. This system will enable those with poor head control to perform head movements using their eyes. The control interface of this system is triggered by the user's pupil motion in a virtual field of view (FOV) to produce head movements. The results indicate that the control interface is capable of rotating the head towards the target within 5° of difference of the desired head angle. This study shows that the proposed bio-inspired control promotes natural eye-head coordination, which may be potentially useful for individuals with poor or limited neck control.**

I. Introduction

We move our head and make eye contact with others during a respectful conversation [1]. However, it is difficult for those with poor head control. Poor head control limits the ability to control and stabilize the movement of the head [2]. In extreme cases, individuals with dropped head syndrome are unable to lift their head against gravity, affecting their interactions with other people [3], [4].

Currently, static cervical collars are the most commonly used devices to keep the head in an upright neutral posture. However, these collars restrict the users to move their head, narrowing the viewing area [3]. To allow a finite range of motion of the head-neck, McDermott et al. developed the 'Sheffield snood' for patients with neck muscle weakness [5]. Douglas et al. used an eye-tracker to control a headrest mounted on a powered wheelchair [6], [7]. Zhang and Agrawal developed a powered wearable neck brace to assist head movement through a joystick [8]. Although this control method was proved to be effective, a subject with limited hand function may have difficulty to use with a joystick.

Eye movement can be a viable alternative to control the head [9]. Existing technologies, such as electrooculography (EOG) and video-based eye trackers, have been used to acquire eye information and control auxiliary assist devices [10], [11]. The main disadvantage of EOG is that any head movement could affect the signal acquired by the electrodes placed on the head. Compared to EOG, video-based eye trackers are more accessible and simple to operate for most people.

[1]Biing-Chwen Chang, Haohan Zhang, and Sunil K Agrawal are with the Department of Mechanical Engineering, Columbia University, New York, NY, 10027 USA bc2700@columbia.edu; hz2347@columbia.edu; sunil.agrawal@columbia.edu

[2]Emilio Trigili is with The BioRobotics Institute, Scuola Superiore Sant'Anna, viale Rinaldo Piaggio 34, Pontedera (PI), Italy. e.trigili@santannapisa.it

Our aim is to design a control method that generates head movement based on natural eye intent. Control of the head is part of the oculomotor system, where the direction of the gaze dictates the pattern of head-eye coordination [12]. Generally, there are two types of eye-head coordination: (i) gaze shift and (ii) smooth pursuit. To make eye contact during a conversation, one commonly initiates a saccade, followed by a head reorientation to trigger the vestibulo-ocular reflex (VOR).

Inspired by this natural behavior, we have created a bio-inspired control interface to enable head-neck movements with natural eye motion. The purpose of this study is to demonstrate the feasibility of this control interface, using eye movements to control our robotic device. A preliminary human experiment is conducted to show the proposed control scheme and the behavior presented in the literature. To our knowledge, this is the first study presenting a bio-inspired eye control strategy to assist head movement. This technology will enable people with poor head control to enhance their social interactions.

II. Bio-inspired Eye-Head Coordination & Control

A. Eye-Head Coordination

Natural eye-head coordination behaviors have been documented in previous studies as humans explore their environment [13], [14]. As shown in Figure 1, eye-head coordination is composed of two parts: saccade and VOR. A saccade is when the eyes glance from one point to another point. VOR follows as the semicircular canals detect the movement of the head. In response to the head movement, the eyeballs make a compensatory movement to stabilize the retinal image. Hence, when a visual or audio stimulus occurs, the eyes perform a saccade after around 0.4 seconds. The head does not rotate with the eyes concurrently. Instead, it starts with a latency of around 0.1 seconds. Then VOR reacts to the head orientation after the gaze fixes on the target at around 0.8 seconds. The final resting position of the head after the saccade and VOR varies from person to person [15]. Yet, both the eyes and the head roughly align with the target. Hence, for individuals who have limited control of the head, we can utilize the characteristics of gaze fixation, vestibular reflex, and the robotic neck brace to develop a natural, bio-inspired motion of the head.

B. Control Interface

Inspired by the mechanism of VOR, i.e., eyes move in a direction opposite to the head during a gaze shift, we propose a control interface to mimic the eye-head coordination. We use a virtual panel fixed relative to the head to represent a

978-1-7281-5907-2/20/$31.00 ©2020 IEEE

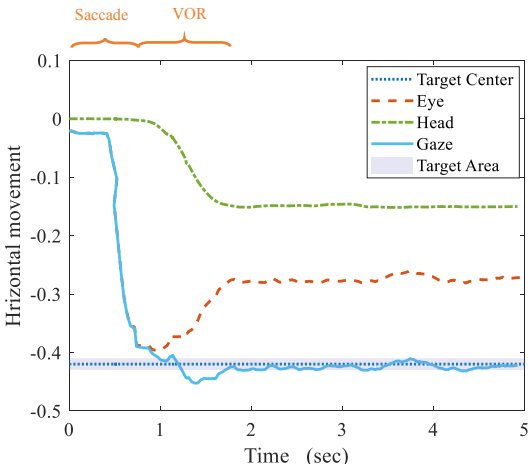

Fig. 1: An example of eye-head coordination when a target appears. We defined the initial virtual field of view (FOV) as the global frame where the subject's head stays neutral, and the eye gaze looks straight ahead. When the head moves, the virtual FOV serves as the local frame. The target, the head, and the gaze are relative to the fixed global coordinate frame, and the eye data is relative to a moving frame fixed to the head. The image captured from the scene camera on an eye-tracker is defined as the virtual FOV to represent the person's FOV. The image is normalized and its coordination is shown in Figure 2. All the values are presented with this coordinate system.

person's FOV. Based on the commonly used head motion, we divide the virtual FOV into five areas, as illustrated in Figure 2. The left and right correspond to the head's axial rotation, while the up and down correspond to flexion-extension. A finite area of the neutral zone allows the eyes to explore around without actuating the brace. Therefore, when the user looks at an object at the left, the gaze would shift to the left to fixate on the target. The line of sight will fall into the left labeled region of the panel and will mark the intent of the head (Figure 2). The neck brace will follow the command and rotate the head to the left. At the same time, the gaze in the virtual FOV would go right towards the neutral zone.

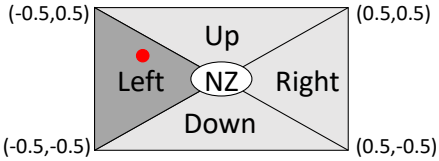

Fig. 2: A virtual panel to control head movement. The panel is divided into five areas where each area represents a direction of movement. NZ is the neutral zone in the center of the area. The red dot denotes the gaze point in the virtual FOV. When the gaze point is within one of the four other regions, the algorithm rotates the head. Once the gaze point is within the neutral zone again, the brace motion stops and then allows the user to explore locally around the neutral position.

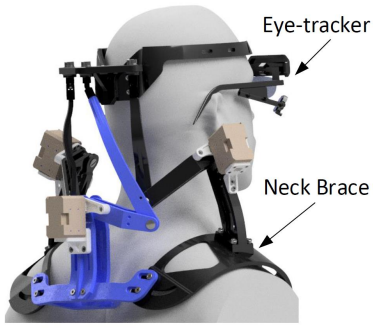

Fig. 3: Schematic of the brace-tracker system.

III. Human Experiment

A. Hardware

The eye-head system consists of a head-mounted eye-tracker (Pupil Labs, Berlin, Germany) and a robotic neck brace, as shown in Figure 3. There are three cameras mounted within the eye-tracker—a scene camera which covers 100° diagonally representing the FOV of a user and two infrared eye cameras that detect the two pupil movements with an accuracy of $1.5^{\circ} - 2.5^{\circ}$. Once calibrated, each eye camera gives an estimate of the gaze point in the world image [16]. The accuracy of the pupil detection within the calibrated area is 0.6°. A numerical value between 0 and 1 is returned that indicates the confidence of measurement of the eye cameras. The resolution of the scene camera is 1280×720 pixels. The output eye data was normalized by the eye tracking software to match the size and the camera intrinsic of the image.

The neck brace has been validated through a series of studies [8], [17]. This parallel robot consists of a base that rests on the shoulder, a soft headband as the end-effector, and three revolute-revolute-spherical chains. Three servomotors (Dynamixel XM430-W350-R, ROBOTIS, Seoul, South Korea) mounted on the inertial base are used to actuate the brace. The brace is programmed by an onboard microcontroller (myRIO-1900, National Instruments, Austin, Texas, USA) and powered by batteries. The full system, including electronics, weighs less than 1.5 kg. The eye-tracker can wire to a mobile phone and transmit data wirelessly to a host computer through network. To ensure reliable data transmission in the experiment, we connected the eye-tracker to a host computer directly through a USB cable.

Combined with eye-tracking and position control from the brace, a schematic of the system is shown in Figure 4. The gaze position can be thought of as being composed of eye position in the head coordinate frame and head position relative to the shoulder coordinate frame. The eye tracker worn by the participant gives the location of the line of sight in the virtual FOV. The eye data is filtered through a threshold algorithm to exclude false pupil detection. The virtual panel converts the data into a directional command. The inverse kinematics of the brace is used to calculate the joint angles for each motor. These angles are passed to a PID controller of the neck brace to update the head position to a new position.

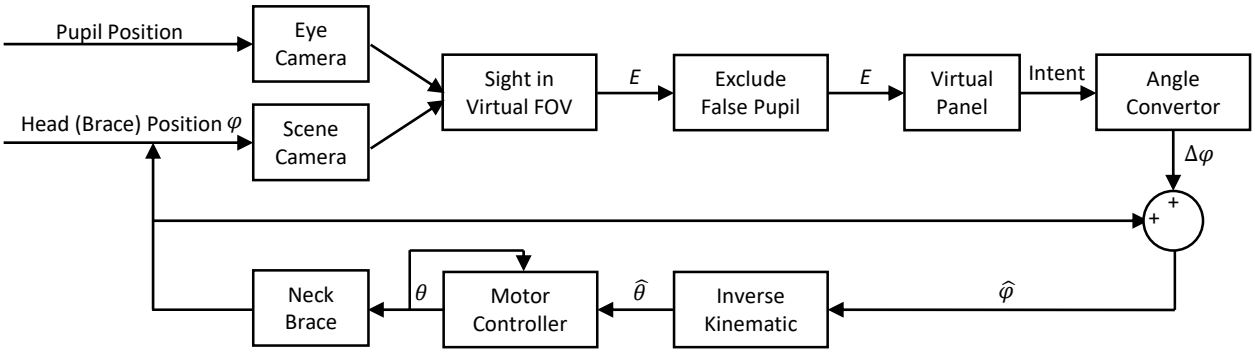

Fig. 4: System schematic diagram. The position of eye gaze E in virtual FOV is obtained from the normalized scene image that is updated with the actual head movement φ and pupil positions. Given a gaze location in the image, after excluding the false pupil detection, the intent is generated through the virtual panel and converted for the incremental angle of $\Delta\varphi$. The desired orientation $\hat{\varphi}$ is then computed using the inverse kinematics to obtain the angular commands to the motors, $\hat{\theta}$. The actual motor angles, θ, are regulated by a PID controller for each motor.

TABLE I: Subject Characteristics

	Mean	Standard Deviation	Range
Age (y)	28.38	3.07	24 - 32
Height (cm)	177.0	7.54	166 - 184
Weight (kg)	82.50	15.15	63 - 110

The brace allows 3D rotations of the head while the gaze location is defined by two coordinates in the scene image. As a result, we prescribe the head orientation only about the vertical and horizontal axes, i.e., flexion-extension and axial rotation. The lateral bending of the head is suppressed when commanding the head movement. This allows mapping a Cartesian point in the scene to flexion-extension and axial rotation of the head-neck.

Blinking or when the position of the pupil is at the peripheral region of eyes may result in low confidence values in the eye-tracker. We choose a confidence value higher than 0.7 as the threshold to exclude poor pupil detection. Once the gaze data is acceptable, it is labeled to belong to one of the five regions. The controller executes these labels every 20 milliseconds. The head motion is executed with a predefined increment of 0.4. This step size is set to be 0.4°/command, or 20°/second.

B. Procedure

To evaluate this eye control interface, we conducted a preliminary human experiment with healthy individuals. In this experiment, we asked subjects to perform natural eye movements without performing voluntary head movements while wearing the device. The control interface would orient the head towards the goal position. The elliptic shape and size of the neutral zone were decided based on the center of vision of human FOV [18].

We recruited eight healthy young adults in this experiment (Table I) approved by the Columbia Institutional Review Board (IRB). The participants were seated with their back layed on a vertical backrest during the experiment (Figure 5). All individuals completed the task three times.

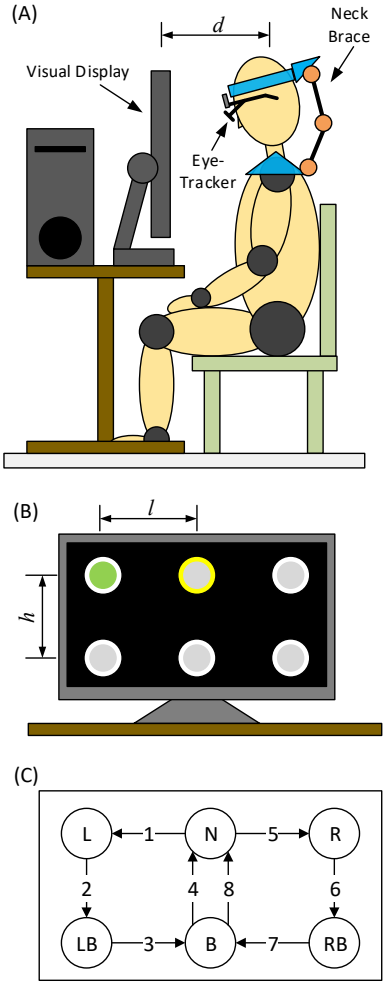

Fig. 5: Experimental setup. (A) Illustration of a user sitting in front of a screen at a distance d (45 cm) during the experiment. (B) Details of the visual display from a user perspective. The visual targets are separated with a width l (18.75 cm) and a height h (15.0 cm). (C) Labeled targets consist of eight moves following the numbered arrows.

There were six targets displayed on a computer screen in front of the subject (Figure 5). At the beginning of the experiment, the eye cameras were adjusted to ensure that they covered the full range of eye movements. The scene camera was placed so that the center of the scene image aligned with the actual gaze point at neutral. The distance between the screen and the subject was 45 cm. We adjusted the height of the screen so that the center of FOV aligned with the top middle target when the head was at the neutral position. Based on our experiment set up in Figure 5, the desired head angles to align with the targets would be 22.61° in the horizontal direction and 17.10° in the vertical direction.

The experiment began with the top middle target illuminated. At this moment, the head of the subject was aligned with this target in a self-reported upright neutral posture. After this, the next point lighted up and turned green in a sequence for the subject to track (Figure 5). The next target would not light up until the participant completed the move to the previous target. Once the subject successfully keeps the head at the current spot for 2 seconds, i.e., the gaze points in the neutral zone, the next target would light up and the current target would switch off.

C. Performance Evaluation

The raw data in each trial was segmented based on the time when each target was lighted. The eye location in the virtual FOV, the intention of the subject, and the encoder data of the servomotors at a given time were synchronized and collected. The orientation of the brace was computed using the joint angle from the encoder data and the forward kinematics of the device structure [19]. Based on the experiment, subjects had to reach the goal to trigger the next target. Hence, we characterized the performance by the completion time to the target and angle change to the next target. Additionally, we calculated command response rate as the percentage of total move to the target.

IV. Results

We first explain the observations using data from a representative subject. This is followed by the group performance data.

A. Representative Data

Figure 6 shows the line of sight and head position of a subject after the saccade and at the end when all movements are stabilized. The goal was to move horizontally, i.e., execute head rotation. The brace rotated the subject's head gradually according to the command received. Eventually, it stopped at the orientation when the gaze was in the neutral zone.

To investigate if the control system provides the motion pattern similar to VOR described in the previous section (Figure 1), we reconstructed the eye-head movement and display in Figure 6. We used video recording from the scene camera to retrieve the eye-head coordination and present in Figure 7. We observed that the saccade happened at 0.34 seconds after the target appeared. The gaze shifted rapidly to this fixed point in 0.10 seconds. Before the brace began to

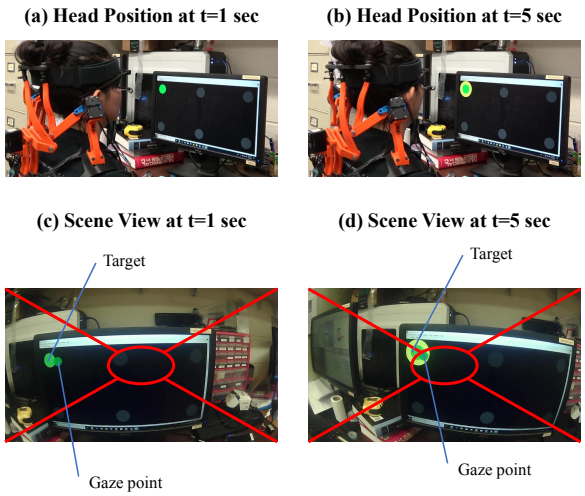

Fig. 6: The start and end position of the eyes and the head during a single step movement (from target N to L). (a) and (b) display where the head was in the first and the fifth second. (c) and (d) display where the gaze is located in the virtual FOV in the first and the fifth second. The large circle is the target where the subject was instructed to look and the small circle is the eye gaze in the virtual FOV. The red frame presents how the virtual FOV is divided into five regions. Once the goal is achieved, i.e., the gaze falls in the neutral zone again, the yellow circle lights up.

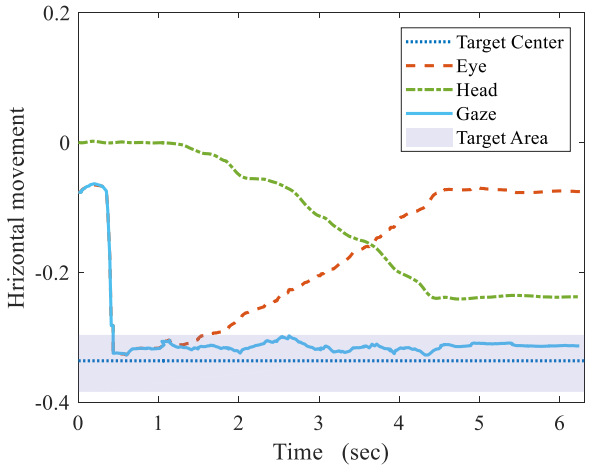

Fig. 7: Eye and head motion for a target horizontal move from N to L from a representative subject. We defined the initial virtual FOV from the scene camera recording as the global frame where the subject's head stays neutral and the eye gaze looks straight ahead. The origin is at the center of the frame, as illustrated in Figure 2. When the head moves, the virtual FOV serves as the local frame. The target, the head, and the gaze are relative to the global coordinate frame, and the eye data is relative to the local coordinate frame. The position of the target center with the shaded area in the virtual FOV served as the goal for the gaze.

turn the head, the trajectory of the gaze was along the line of sight. VOR then engaged in the eye movement to maintain the fixation of the gaze while the head was rotating.

B. Group Results

All subjects were able to complete the sequence of eight moves within one minute and a half. We first determined that all subjects were performing VOR with assistance from the brace. Then, we showed that the brace stopped when they achieved the target, i.e., the line of sight was in the neutral zone. Figure 8 shows the average head angles of the group at each step when the brace stopped. Compared to estimated values for each target, we found that the steady-state head position after step 1 had a mean overshoot of 3.95°. The subjects were 5.00° short of the ideal angle after step 5. The steady-state head angles in the vertical directions were greater than the estimated angles, but within 2.00°. Table II presents a chart of subjects' performance. The group average completion time to left, right, up, and down directions were higher than the estimated completion times. Additionally, the group average incremental step sizes were lower than the default step size of 0.4°/command. We found that there was a consistent 0.04 seconds delay from intent generated by eye data to the command in the brace control. Additionally, the motor reacted $0.08 \sim 0.12$ seconds later after receiving the command. Furthermore, the brace did not successfully generate the corresponding output angle for some of the commands, resulting in a lower group average command response rates.

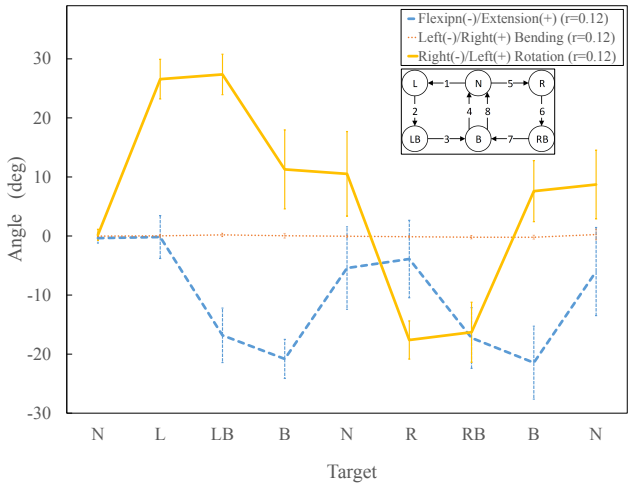

Fig. 8: The group mean and standard deviation of head angles at each target in 3-dimensions after the brace stopped at each step. The sequence and the target positions are also presented.

V. Discussion

In this study, we demonstrated the feasibility of the bio-inspired eye-head controller. The experiment results show that all subjects were able to use the system to mimic general eye-head coordination behavior, as shown in Figure 6. The completion times were longer in the horizontal direction than in the vertical direction. The error of 5.00° was observed in both horizontal and vertical directions.

TABLE II: Subject Performance

Direction	Completion Time (sec)	Step Size (°/command)	Command Responding Rate (%)
Left	3.22(1.94)	0.17(0.06)	73.0
Right	2.25(1.21)	0.20(0.07)	76.3
Up	1.43(0.85)	0.20(0.05)	84.0
Down	1.75(1.90)	0.21(0.07)	78.2

The performance of the system and parameters of the current controller affected both the completion time and head angles. Lower command response rate added up the total completion time. Also, the time delay between the eye input and brace angle output produced a larger head rotation, leading to longer completion time and overshoot of the head angle. Additionally, our experiment task design and the presence of the neutral zone caused the angle differences between the desired and the actual head angles. The design of the neutral zone was to mimic this natural behavior by stopping the brace when the line of sight entered the neutral zone. When individuals intended to turn the head towards the opposite direction, the head angle change is smaller because part of the line of sight movement is within the neutral zone.

The significance of this work is to demonstrate the concept of controlling the head motion by the gaze intuitively, showing the potential of head motion assistance in daily living. Being able to control head is important, especially when interacting with other people. Although the snood [5] solved the head drop issues by fixating the head to an upright posture, lacking freedom of the neck still leads to fatigue and social isolation overtime. Also, when the individual intends to look at objects at the side, it is uncomfortable for the user if the pupil stays in the peripheral area of the field of view over a long period of time [20]. Hence, previous studies used a joystick to control the robotic neck brace [8]. The study showed that neck muscles activated less when the user was controlling the brace to assist the movement. This method is sufficient when the patients' hands are functional. However, this method is not suitable for patients who have lost their hand function. Additionally, it requires users to learn how to use their hands to control head rotation in three axes. With our current controller, the brace rotates the head towards the object by using the intent of the eyes.

In this study, we showed the feasibility of the proposed controller. However, there are several variables and parameters which could be further investigated to improve the controller. The first is to include the head position in the control loop. People prefer their head to stay in a neutral position. The current controller did not take into account when the gaze was fixating at the center target. Also, the velocity of the brace can be proportional to the eccentricity of the target. Freedman had shown that the peak head velocity increases when the target is further away from the center [13]. Possible solutions are to add radial levels in the virtual panel or use the vector length and direction of the line of sight to assign different speeds for the brace. Additionally, the size and the shape

of the neutral zone could be customized based on subjects. Finally, we could investigate if the system enables people to perform smooth pursuit or other nonverbal head gestures often used in a conversation.

Another direction to improve the controller's performance is to use machine learning to characterize the behavior and implement it on the system. From the literature, we know that even with the same eye-head coordination mechanism, there is variance among people, such as head movers and non-head movers [21]. Different scenarios also affect the coordination between the head and eyes. Recognizing the fixating objects from the scene camera image and classifying the corresponding head movement may improve the controller's ability to produce a more natural movement. Besides relying on previous literature, observation experiments with the brace worn by healthy individuals could help understand the interaction between the user and the device, and involving machine learning could build a more robust controller based on user characteristics.

VI. Conclusion

This paper presented a novel approach to control a robotic neck brace by using observed natural eye-head behavior. The main contribution of this study is to use the vestibulo-ocular reflex to control the head intuitively. This approach uses the eye movement as an input to rotate the robotic neck brace incrementally. Also, the control interface allows the user to explore around when the gaze is within the neutral zone of the field of view. The system provides both a hands-free and screen-free user interface. The experiment demonstrated the ability to use this system by imitating the head and eye coordination during social interactions. Several other parameters, such as the speed of the brace, the size and the shape of the neutral zone, could be customized to improve the performance of the system.

Acknowledgment

This work was supported by National Science Foundation (Grant No. IIS-1527087).

References

[1] D. Heylen, "Head gestures, gaze and the principles of conversational structure," *International Journal of Humanoid Robotics*, vol. 3, no. 03, pp. 241–267, 2006.

[2] A. Z. Burakgazi, P. K. Richardson, and M. Abu-Rub, "Dropped head syndrome due to neuromuscular disorders: Clinical manifestation and evaluation," *Neurology international*, vol. 11, no. 3, 2019.

[3] T. G. Petheram, P. G. Hourigan, I. M. Emran, and C. R. Weatherley, "Dropped head syndrome: a case series and literature review," *Spine*, vol. 33, no. 1, pp. 47–51, 2008.

[4] M. Gourie-Devi, A. Nalini, and S. Sandhya, "Early or late appearance of "dropped head syndrome" in amyotrophic lateral sclerosis," *Journal of Neurology, Neurosurgery & Psychiatry*, vol. 74, no. 5, pp. 683–686, 2003.

[5] S. Pancani, J. Rowson, W. Tindale, N. Heron, J. Langley, A. D. McCarthy, A. Quinn, H. Reed, A. Stanton, P. J. Shaw *et al.*, "Assessment of the sheffield support snood, an innovative cervical orthosis designed for people affected by neck muscle weakness," *Clinical Biomechanics*, vol. 32, pp. 201–206, 2016.

[6] G. Douglas, E. Guld, M. Hewett, and F. Macdonald. (2010) Motorized headrest for people with neck muscle weakness. [Online]. Available: https://sites.psu.edu/resnasdc/2010/05/13/motorized-headrest-for-people-with-neck-muscle-weakness-the-university-of-british-columbia/

[7] F. Macdonald, E. Guld, and C. Hennessey, "A study of applying gaze-tracking control to motorized assistive devices," *CMBES Proceedings*, vol. 33, 2010.

[8] H. Zhang and S. K. Agrawal, "An active neck brace controlled by a joystick to assist head motion," *IEEE Robotics and Automation Letters*, vol. 3, no. 1, pp. 37–43, 2018.

[9] A. T. Duchowski, "Eye tracking methodology," *Theory and practice*, vol. 328, p. 614, 2007.

[10] G. Norris and E. Wilson, "The eye mouse, an eye communication device," in *Proceedings of the IEEE 23rd Northeast Bioengineering Conference*, May 1997, pp. 66–67.

[11] S. Crea, M. Nann, E. Trigili, F. Cordella, A. Baldoni, F. J. Badesa, J. M. Catalán, L. Zollo, N. Vitiello, N. G. Aracil *et al.*, "Feasibility and safety of shared eeg/eog and vision-guided autonomous whole-arm exoskeleton control to perform activities of daily living," *Scientific reports*, vol. 8, no. 1, pp. 1–9, 2018.

[12] F. A. Proudlock and I. Gottlob, "Physiology and pathology of eye–head coordination," *Progress in retinal and eye research*, vol. 26, no. 5, pp. 486–515, 2007.

[13] E. G. Freedman, "Coordination of the eyes and head during visual orienting," *Experimental brain research*, vol. 190, no. 4, p. 369, 2008.

[14] F. A. Proudlock, H. Shekhar, and I. Gottlob, "Coordination of eye and head movements during reading," *Investigative ophthalmology & visual science*, vol. 44, no. 7, pp. 2991–2998, 2003.

[15] J. S. Stahl, "Amplitude of human head movements associated with horizontal saccades," *Experimental brain research*, vol. 126, no. 1, pp. 41–54, 1999.

[16] M. P. Kassner and W. R. Patera, "Pupil: constructing the space of visual attention," Ph.D. dissertation, Massachusetts Institute of Technology, 2012.

[17] H. Zhang, B.-C. Chang, and S. Agrawal, "Using a robotic neck brace for movement training of the head-neck," *IEEE Robotics and Automation Letters*, 2019.

[18] H. Strasburger, I. Rentschler, and M. Jüttner, "Peripheral vision and pattern recognition: A review," *Journal of vision*, vol. 11, no. 5, pp. 13–13, 2011.

[19] H. Zhang and S. K. Agrawal, "Kinematic design of a dynamic brace for measurement of head/neck motion," *IEEE Robotics and Automation Letters*, vol. 2, no. 3, pp. 1428–1435, 2017.

[20] M. Menozzi, A. v. Buol, H. Krueger, and C. Miege, "Direction of gaze and comfort: discovering the relation for the ergonomic optimization of visual tasks," *Ophthalmic and Physiological Optics*, vol. 14, no. 4, pp. 393–399, 1994.

[21] J. H. Fuller, "Head movement propensity," *Experimental Brain Research*, vol. 92, no. 1, pp. 152–164, 1992.